Weather and Climate Extremes 29 (2020) 100259

Contents lists available at ScienceDirect

Weather and Climate Extremes

journal homepage: http://www.elsevier.com/locate/wace

The role of spatial and temporal model resolution in a flood event storyline approach in western Norway

Nathalie Schaller [a,*], Jana Sillmann [a], Malte Müller [b], Reindert Haarsma [c], Wilco Hazeleger [d], Trine Jahr Hegdahl [e], Timo Kelder [f], Gijs van den Oord [g], Albrecht Weerts [h,i], Kirien Whan [c]

[a] Center for International Climate Research (CICERO), Gaustadalleen 21, 0349 Oslo, Norway
[b] The Norwegian Meteorological Institute, Postboks 43 Blindern, 0371 Oslo, Norway
[c] Royal Netherlands Meteorological Institute (KNMI), De Bilt, the Netherlands
[d] Faculty of Geosciences, Utrecht University, Heidelberglaan 8, 3584 CS Utrecht, the Netherlands
[e] Norwegian Water Resources and Energy Directorate (NVE), Middelthuns Gate 29, 0368 Oslo, Norway
[f] Geography and Environment, Loughborough University, Loughborough, UK
[g] Netherlands eScience Center, Science Park 140, 1098 XG Amsterdam, the Netherlands
[h] Deltares, Postbus 177, 2600 MH Delft, the Netherlands
[i] Hydrology and Quantitative Water Management Group, Wageningen University, Wageningen, the Netherlands

ARTICLE INFO

Keywords:
Storyline approach
Atmospheric river
Extreme precipitation
Flood
Climate change
EC-Earth
AROME
Dynamical downscaling
Western Norway

ABSTRACT

We apply a physical climate storyline approach to an autumn flood event in the West Coast of Norway caused by an atmospheric river to demonstrate the value and challenges of higher spatial and temporal resolution in simulating flood impacts. We use a modelling chain whose outputs are familiar and used operationally, for example to issue flood warnings. With two different versions of a hydrological model, we show that (1) the higher spatial resolution between the global and regional climate model is necessary to realistically simulate the high spatial variability of precipitation in this mountainous region and (2) only with hourly data are we able to capture the fast flood-generating processes leading to the peak streamflow. The higher resolution regional atmospheric model captures the fact that with the passage of an atmospheric river, some valleys receive high amounts of precipitation and others not, while the coarser resolution global model shows uniform precipitation in the whole region. Translating the event into the future leads to similar results: while in some catchments, a future flood might be much larger than a present one, in others no event occurs as the atmospheric river simply does not hit that catchment. The use of an operational flood warning system for future events is expected to facilitate stakeholder engagement.

1. Introduction

Between the 27th and 29th of October 2014, large amounts of precipitation - up to 300 mm in less than 5 days in some areas - fell over the West Coast of Norway, causing floods and damages in several valleys (Lussana et al., 2018). The towns of Flåm and Odda were particularly affected, with bridges destroyed and houses dragged into the river. The West Coast of Norway is the wettest region in Europe (e.g. Lussana et al., 2018) and due to its steep topography (see SI Fig. 1), often experiences floods. Spring floods are usually associated with snow melt, summer floods with convective precipitation and autumn floods with atmospheric rivers (Dyrrdal et al., 2016). The large amounts of rain in October 2014 were caused by the passage of such an atmospheric river (Lussana et al., 2018 and SI Fig. 2a). Atmospheric rivers are long and narrow regions of intense water vapour transport in the lower atmosphere and Sodemann and Stohl (2013) and Azad and Sorteberg (2017) have shown how important they are to transport sub- and extratropical moisture to the West Coast of Norway. Benedict et al. (2019a) further showed that atmospheric rivers are associated with more than 85% of extreme precipitation in this region for the period September–March from 1979 to 2014.

But even in a region used to heavy precipitation and floods, it is a challenge to decide what (and to what extent) adaptation measures should be considered for the future, when even more precipitation is projected by climate models (Whan et al., 2019). Making sense of and using probabilistic climate projections for extreme weather events is

* Corresponding author.
E-mail address: thalie.schaller@gmail.com (N. Schaller).

https://doi.org/10.1016/j.wace.2020.100259
Received 9 December 2019; Received in revised form 23 April 2020; Accepted 11 May 2020
Available online 8 June 2020

challenging for most decision makers and end-users (Porter and Dessai, 2017). One of the main issues is the coarse resolution, both in a space and time, provided by Global Coupled Models and Regional Coupled Models (GCMs and RCMs), which is often not adapted to the user needs. Another difficulty lies in the interpretation of the model output, especially the often large ranges of outcomes obtained when combining different GCMs and RCMs, while users seem often to prefer a single value with a probability attached to it. Probabilistic climate projections are certainly the basis of our knowledge on future climate change and its uncertainties, but there is a growing demand for climate change information that is more relevant, useful and tailored to user needs, especially on the topic of climate impacts (Shepherd et al., 2018). Bottom-up approaches, where a study is designed with users and their needs discussed upfront, rather than climate scientists assuming what information is useful, are to be favored (Dee et al., 2011).

Storyline approaches, where "tales" about possible future weather events are created, are currently being advanced as a way to complement information from the more classic probabilistic assessments and to better feed the imagination of users (Hazeleger et al., 2015). Physical climate storylines are physically self-consistent unfolding of past events, or of plausible future events, which are conditioned on a set of assumptions and built from causal arguments, but mainly inspired by observed or anticipated high impact events. They are particularly designed to improve risk awareness, to strengthen decision-making (e.g. proactive adaptation), to explore the boundaries of plausibility, and to provide a physical basis for partitioning uncertainty (Shepherd, 2019).

Since in a physical climate storyline study, the focus is on specific events with limited spatial and temporal scope, the computational requirements are smaller in terms of numbers of time steps, climate models and ensemble members used, and therefore higher resolution versions of a climate model can be more easily run. However, one needs to decide how to constrain the simulations for a specific event. The assumption is that by having a higher resolution in both time and space, and ideally, data formats already known by the user, or used operationally, will provide more relevant information for users as this level of detail cannot be achieved currently in a full probabilistic context given computing limitations (Hegdahl et al., 2020).

A key aspect of a physical storyline is therefore the modelling chain used. Recently, studies have reported successful coupling of several models beyond the established GCM-RCM-hydrological model chain. For example, Felder et al. (2018) demonstrated the feasibility of a full and comprehensive model chain from the atmospheric to local scale flood loss models. In the context of probabilistic event attribution, Schaller et al. (2016) went from GCM simulations of the particular weather situation during the 2013/2014 winter over the North Atlantic/British Isles to the count of properties at risk of flooding in the Thames catchment. While probabilistic event attribution compares extreme events in the present versus the same extreme event in an alternative present where there would have been no human influence, physical climate storyline approaches attempt to translate an extreme event that has happened and is of interest to users into the future, where some level of human activity is assumed in terms of anthropogenic GHG emissions and/or socio-economic changes (e.g. different management practices) (Shepherd et al., 2018; Sillmann et al., 2019). Both research fields, probabilistic event attribution and physical climate storylines, could benefit from the other by lessons learned as they develop. For example, in the case of flood events, it is key to at least use one hydrological model rather than stopping at the heavy precipitation event. Each river catchment has very specific properties that cannot be generalized, and in some cases, even if a signal is found from the GCMs and RCMs, it could be diluted at the hydrological model step, as in Schaller et al. (2016).

The overall aim of this study is to investigate how a high-impact extreme event in the future would look like compared to one in the present climate, using a physical climate storyline approach and an operational modelling chain.

As mentioned above, there is an assumption that physical climate storyline approaches, with their higher spatial and temporal resolutions, provide an added value compared to more standard probabilistic multimodel/multi-scenario approaches such as, e.g., the Coupled Model Intercomparison Project Phase 5 (CMIP5, Taylor et al., 2012) or the European Coordinated Regional Downscaling Experiment (EURO-CORDEX, Jacob et al., 2014) (Hazeleger et al., 2015). This seems particularly relevant in the case of floods associated with extreme precipitation in a mountainous region such as the West Coast of Norway, as indicted in e.g. Müller et al., 2017; Prein, 2015. In addition, climate information can best be used by users when it is provided in a format they are familiar with. In this study, we are therefore using the operational modelling chain for flood forecasting in Norway to show the effect of having higher temporal and spatial resolution models on the simulated streamflows.

Section 2 describes the methods used for the event selection and model simulations performed. In Section 3, we compare the simulated and actual events, and put the differences between the present and future events into the context of global warming. Then we present and discuss the effect of higher spatial and temporal model resolution to simulate streamflows in specific catchments, and present conclusions in Section 4.

2. Methods

2.1. Stakeholder involvement and event selection

The Norwegian Meteorological Institute and Statkraft (the largest energy provider in Norway) are stakeholders directly involved in the project and provided insights for the event selection. During the kick-off meeting of the project at the end of 2016, different extreme events that occurred in Norway in the recent past were further discussed with a larger group involving further stakeholders, such as municipalities, television channels and state authorities (https://www.cicero.oslo.no/en/posts/single/making-sense-of-future-climate). The events that sparked most interest were the September 2005 and October 2014 floods hitting western Norway, and particularly causing severe damages in the city of Bergen and the touristic fjord village Flåm, respectively (Iden et al., 2005; Lussana et al., 2018; Stohl et al., 2008). For this reason, the analogue event considered in this study is an October flood caused by an atmospheric river (AR).

The premise of this study is to use an existing and operational modelling chain to ease the use of the results to the different potential users. The Norwegian Meteorological Institute uses the 6-hourly short range weather forecast from the ECMWF model, downscales them using the AROME-MetCoOp model for Scandinavia, and the output is used by the state meteorologists to issue weather forecasts, but also by the Norwegian Water Resources and Energy Directorate (NVE), to issue flood warnings. We run two different hydrological models that use different temporal and spatial input from the weather forecast to show the added value for the users of having high resolution climate and hydrological models. The rest of this section describes in more details the different types of models (i.e. global climate model, regional weather forecasting model and hydrological models) used to reproduce as closely as possible the operational setup for weather forecasts and flood warnings in Norway.

2.2. The EC-Earth high-resolution global climate model and AR events

2.2.1. EC-Earth control simulations

The global climate model used is EC-Earth v2.3 model (Hazeleger et al., 2010) at a resolution of T799 L91 (~25 km), which was the operational resolution at the European Centre for Medium Range Weather Forecasts (ECMWF). This spatial resolution is much higher than in any of the CMIP5 models (Taylor et al., 2012) and is able to resolve tropical cyclones (Haarsma et al., 2013). Different model runs were

performed for the present (2002–2006) and future (2094–2098) climate, which are referred to as EC-Earth PRESENT and FUTURE in the rest of the text. Each of these datasets consists of a 6-member ensemble spanning 5 years resulting in a 30-year dataset. In present simulations, observed greenhouse gas and aerosol concentrations were applied while future concentrations were derived from the RCP 4.5 scenario (van Vuuren et al., 2011). Only the atmosphere and land surface (HTESSEL; van den Hurk et al., 2000) are solved explicitly by the model to allow for the generation of high-resolution results spanning an extensive period of time. Therefore, sea surface temperatures (SSTs) were imposed using daily data at 0.25° resolution from NASA (http://www.ncdc.noaa.gov/oa/climate/research/sst/oi-daily.php) for the 2002–2006 period. An estimate of the SST for the other periods was made by adding the ensemble mean predicted change using ECHAM5/MPI-OM in the ESSENCE project (Sterl et al., 2008) which used the SRES A1B scenario. This is comparable to RCP 4.5 scenario, having a slightly larger global temperature increase by the end of the twenty first century (Rogelj et al., 2012; Haarsma et al., 2013). The 5 independent ensemble members were generated by small perturbations of the atmospheric initial conditions; for further details on this model setup and spin-up we refer to Haarsma et al. (2013) and Benedict et al. (2019b). The output data was stored on 5 pressure levels (850, 700, 500, 300 and 200 hPa) at 6-hourly intervals, surface fields were saved on 3-hourly basis. For each member a restart state was saved on the first of January of every simulated year, ensuring bit-exact reproducibility of the generated weather at the computing facility at KNMI.

2.2.2. Selection of AR events in EC-Earth in present and future climate

The sum of the large scale and convective precipitation fields produced by EC-Earth served as the basis for the analysis of extreme rainfall events. The daily cumulant of this quantity within the West Coast region provided the distribution of which the days above 99.98 percentile were selected. This translates to a lower bound of 77 mm/day for the present day and 89 mm/day for the future climate datasets. This percentile was chosen to yield two events for each period. Of the two events in the present, one occurred in October and the other in November, and in the future, one occurred in October and one in January. To avoid potential inconsistencies with precipitation falling as snow in November and January, we chose only the October events in both present and future.

A brief model evaluation of these EC-Earth simulations for the month of October is presented in SI Fig. 2, since this is the month in which the selected events occur. Haarsma et al. (2013) however provide a more formal evaluation of the model. Whan et al. (2019) further found that EC-Earth has a good representation of the annual cycle of AR frequency compared to ERA-Interim (Dee et al., 2011), with most events occurring in September to January. The number of AR events per year in ERA-Interim and EC-Earth is also very similar.

2.3.3. Perturbation of AR events in EC-Earth

After the event selection described above, we have used the same EC-Earth binary to generate 10-member 'forecast' ensembles for each of these events (referred to as EC-Earth reruns in the following). From the existing restart states, we ran the model until 5 days before the precipitation peak and let it write a new restart state. Because we used the exact restarts on the same machine, we were able to identically recreate the selected events. Then, from these snapshots 10 ensemble members are created using stochastically perturbed parametrization tendencies (SPPT) in the Integrated Forecasting System. This method adds multiplicative noise to the model physics tendencies, representing the arbitrariness of the model's subgrid parametrization schemes:

$$X_{tot} = X_{dyn} + (1+\rho)X_{phys}$$

where X_{tot} denotes the total tendency, X_{dyn} the tendency from explicit dynamics and X_{phys} arises from vertical model physics such as radiation, clouds, convection and turbulence. All prognostic variables (wind components, temperature and humidity) are subject to this randomization and ρ are random numbers on a latitude-longitude grid of 2.5° x 2.5° which are re-generated every 5 time steps, i.e. 50 min. Within each of these grid boxes, the multiplicative noise on the physics tendencies is uniformly distributed within the interval $-0.5 < \rho < 0.5$. For these members we used the same SST and aerosol and greenhouse gas forcings as for the original datasets. The procedure results in an ensemble of 10 global runs which all give rise to atmospheric rivers and high precipitation rates at the selected event dates. These members were run for 7 days to capture the full event and all prognostic fields were saved on all model levels for downscaling purposes. Because we chose a moderate perturbation of the tendencies and started only 5 days before the occurrence of the extreme event, the members are correlated and display all high precipitation rates at the event date.

2.3. The regional operational weather forecast model AROME-MetCoOP

The regional weather prediction system AROME-MetCoOp (Müller et al., 2017) used for the operational weather forecast in Norway, is used here to downscale the atmospheric simulations from EC-Earth. The AROME-MetCoOp model covers large parts of the Nordic countries with a horizontal resolution of 2.5 km, on a 750 by 960 grid, and with 65 layers in the vertical where the lowest level is at 12 m. The model has non-hydrostatic dynamics, semi-Lagrangian advection and two-time level semi-implicit time stepping using a 75 s time step. Parameterisation of physical processes are described in Bengtsson et al. (2017). AROME-MetCoOp is a particular configuration of the HARMONIE system suited for the highest resolutions. HARMONIE (Hirlam Aladin Regional/Meso-scale Operational NWP In Europe) is a cooperation including Meteo-France and their Aladin partners, the Hirlam group and also ECMWF with their IFS (Integrated Forecasting System) model. The configuration used in this study (harmonie-40h1.1.rc.1) is very close to the operational weather forecasting version used in MetCoOp in early 2018.

The AROME-MetCoOp operational weather prediction system (referred to as AROME in the following) has been evaluated in detail in Müller et al. (2017) and they showed that forecasting of precipitation is strongly improved compared to the global ECMWF weather prediction system (horizontal resolution T1279, approx. 16 km), which is used as input for AROME in the operational weather forecast for Norway. Especially, during extreme events of large-scale precipitation, the magnitudes and locations of maximum precipitation are more consistent with observations.

For this study, AROME is forced by 3-hourly EC-Earth simulations at the lateral and upper boundaries. The model is initialized by the EC-Earth fields 36 h before the extreme event and forecasts up to a lead time of 144 h (6 days) are performed.

2.4. The operational flood forecasting model HBVlump

The Hydrologiska Byråns Vattenbalans (HBV) model (Bergström, 1976) as described in Sælthun (1996) and Beldring (2008) is used by the operational flood forecasting service in Norway. The operational HBV model (in the following referred to as HBVlump) uses daily catchment average values of temperature and precipitation as input. The upstream area of a streamflow measuring point defines the catchment area. Each catchment is divided into ten equally large elevation zones, and the average temperature and precipitation is elevation adjusted to each elevation zone. The model consists of a vertical structure with a soil moisture routine, a snow routine, and response functions for quick and slow runoff.

The HBVlump is calibrated for the 1996–2012 period, and thereafter validated for the 1980–1995 period, using temperature and precipitation from the seNorge v1.1 dataset (Mohr, 2008, 2009) as observed input, and the measured streamflow from the NVE database as a reference. Nash-Sutcliffe efficiency (Nash and Sutcliffe, 1970) and volume

bias are the chosen calibration metrics. In this study, we focus on two catchments, Flåm, which flooded in October 2014, and Røykenes, a catchment representative for the September 2005 flood that affected the city of Bergen. Røykenes has a Nash-Sutcliffe efficiency of 0.82 for the calibration period and 0.81 for the validation, with a volume bias of 10%, whereas Flåm has Nash-Sutcliffe efficiency of 0.82 for the calibration and 0.71 for the validation, with volume bias of 7%..

2.5. The hydrological model HBVdist

A platform for distributed hydrological modelling, wflow_hbv, is used to set up the distributed HBV model (Schellekens et al., 2017). This version of the model, using gridded input data rather than catchment-averaged values, can incorporate geographical information (e.g. elevation, geology and land-use) and solves the water balance for each grid cell. The water balance is solved in the same way as previously described for HBVlump and the resulting quick and slow runoff are forced into a kinematic wave routing model. Pre-processing of the input data is performed in Delft-FEWS (Werner et al., 2013).

The distributed HBV model is calibrated on 1 × 1 km spatial and hourly time resolution. A gridded hourly version of the seNorge v.2.0 dataset (seNorge2 in the following, Lussana et al., 2018) is used to provide observed temperature and precipitation input and hourly streamflow measurements are used as reference. Because the hourly temperature and precipitation series are much shorter than the daily version, the calibration was performed over the period 2010–2013 and the years 2014–2016 were used for validation. No streamflow observations were available for the year 2015 in Flåm because the measurement station was destroyed during the flood in 2014, meaning that there are only two years of data for model validation for this catchment. In consultation with NVE, the parameters representing field capacity ('FC'), snowmelt ('TT'), snow/rainfall partitioning ('TTI'), seepage through the soil layer ('BetaSeepage'), and recession coefficients influencing the slow and quick runoff ('K4' and 'KHQ') were selected as most representative of the dominant characteristics in the Norwegian catchments. These parameters were selected for calibration with similar ranges for the parameters as previously reported in Nordic studies (Swedish Meteorological and Hydrological Institute, 2014).. The python package for parameter estimation (SPOTPY) is used to perform the calibration, with 400 Monte Carlo samples, assuming uniform distribution of the parameters and a spin-up period of two months (Houska et al., 2015). Because of its focus on peaks, Nash-Sutcliffe efficiency is used as objective to compare simulations with observations (Nash and Sutcliffe, 1970). For Flåm, the Nash-Sutcliffe efficiency is 0.67 for the calibration phase and 0.69 the validation period. For Røykenes, the Nash-Sutcliffe efficiency is 0.82 for both the calibration the validation phase.

2.6. Initial hydrological conditions

The HBV model has storages for groundwater, soil-moisture and snow, where especially snow and soil-moisture are important for the development of floods in Norwegian catchments. Since streamflow response depends on the water storage within a catchment, there is consequently not a unique relationship between precipitation intensities and flood sizes (Beldring et al., 2008). To spin up the hydrological models and thereby define the hydrological states the models are run using the seNorge2 interpolated temperature and precipitation observations. The states at the end of the spin-up period are used as initial hydrological conditions for all present and future event simulations.

HBVlump was run with daily observations 1 year prior to 25th October 2014. The states from October 2014 are chosen for two reasons: in October 2014 there were a situation with AR induced floods (Lussana et al., 2018) and in addition, the weather in October 2014 was wet and mild (small snow storages), and therefore similar to what is expected to occur in a future climate in western Norway (e.g. Hanssen-Bauer et al., 2017).

In the HBVdist setup, ten initial conditions are sampled to incorporate variability arising from plausible autumn initial hydrological conditions other than the 2014 event. The HBVdist model was run over the years 2010–2014 and the hydrological model states are selected on the 10th of September and 10th of October. Note that in this approach the same initial conditions are used for the present and future climate, whereas a reduction in the snow reservoir in the future is very likely (Hanssen-Bauer et al., 2017). However, in autumn in Norway, extreme precipitation is the dominant driver of floods (Beldring, 2008) and the amount of snow is still building up and is relatively small, so therefore the overestimation of future initial snow conditions is assumed to be of little importance for the flood magnitude.

3. Results and discussion

3.1. The event - as observed and simulated

The event on the 27th and 28th of October 2014 in Flåm, is shown in SI Fig. 2 using the ERA-Interim reanalysis in terms of integrated water vapour transport (IVT). ARs are objectively identified by applying a detection algorithm based on the IVT field, as described in Whan et al. (2019). The two selected modelled events are shown in SI Fig. 2 b-c. 10 reruns are then performed for each of these two present and future events. As expected, all the reruns also have an AR, however, the location and intensity in terms of IVT varies. SI Fig. 3 further shows that EC-Earth has a small positive bias in terms of IVT over the North Atlantic Ocean in general compared to ERA-Interim but is generally able to represent ARs statistics properly (Whan et al., 2019).

SI Fig. 3 shows that the October climatology in EC-Earth reproduces well different percentiles of daily accumulated precipitation along the West Coast region compared to seNorge2. Despite having different horizontal resolutions (25 km and 2.5 km), both EC-Earth and AROME (see Müller et al., 2017) perform well in terms of precipitation in the West Coast of Norway and are therefore appropriate models to perform this storyline study.

The observed accumulated precipitation in the West Coast region (defined as 60°-61°N, 5.2°-7.5°E) over a 6-day period, from 25th until 30th of October 2014, using seNorge2 is shown in Fig. 1. In the present, the 10 ensemble members from EC-Earth reruns and AROME show similar accumulated precipitation amounts, although the time evolution of the events differs slightly, especially in the first 30 h. The reason for this is that the October 2014 event was characterised by two peaks in precipitation, whereas the events selected in the EC-Earth simulations had a single peak.

Fig. 1 further shows how a future heavy precipitation event also caused by an AR in October could look like in the West Coast region. Overall, the accumulated precipitation after 6 days is larger in these future events compared to the present events, with a few ensemble members in both the EC-Earth reruns and AROME having similar or lower amounts compared to the 2014 event. Especially in the present events, EC-Earth appears wetter compared to AROME. SI Figs. 5 and 6 show maps of 6 days accumulated precipitation for the present and future events in all ensemble members. From these maps, it is clear that AROME does simulate higher local peaks, but also many areas in-between with very little precipitation, whereas EC-Earth is wet in every grid cell. This is likely the reason why, when looking at a larger area such as the West Coast region defined here, a coarser resolution model might appear wetter. This result shows that using a high-resolution regional atmospheric model such as AROME is beneficial to give a more realistic and more complete picture of the chance of a catchment being hit. Using a high-resolution GCM will indicate that the passage of an atmospheric river leads to precipitation in each grid cell, which is not according to observations. The localised nature of precipitation is something that users experience every day, so using a higher resolution regional model that reproduces this characteristic should give

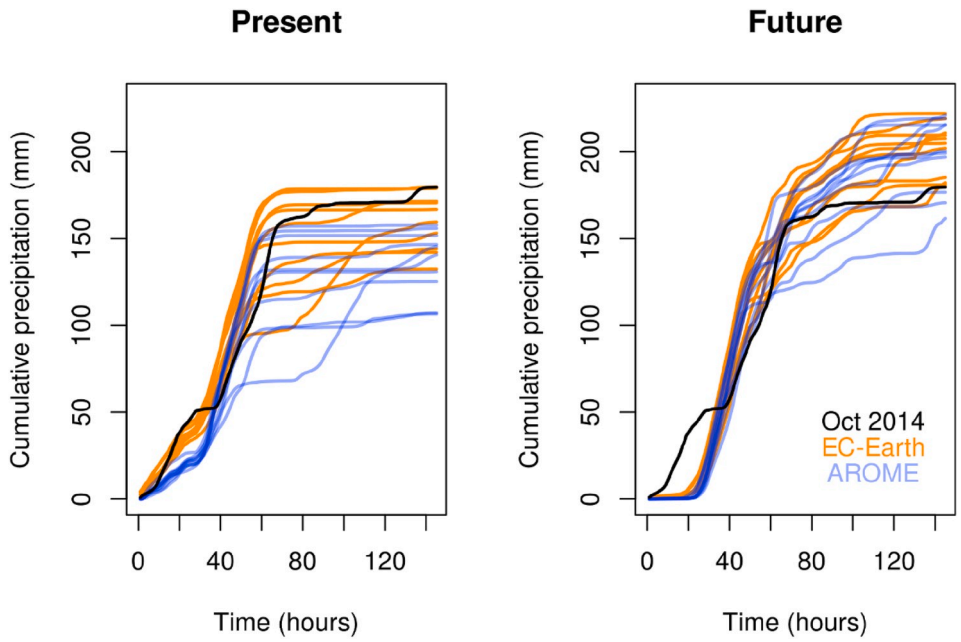

Fig. 1. Cumulative distribution of precipitation during the October 2014 event in seNorge2 (black) and each of the ten ensemble members of AROME (blue) and EC-Earth (orange) in the present (left) and future (right), for the region in 60°-61°N, 5.2°-7.5°E. (For interpretation of the references to colour in this figure legend, the reader is referred to the Web version of this article.)

more trust in the story.

To put these results in context, extreme and mean precipitation are expected to increase both during the cold and warm season in Northern Europe according to the CMIP5 models (Hodnebrog et al., 2019; Sillmann et al., 2013). However, when using a higher resolution model (WRF driven by CESM1-CAM4), Hodnebrog et al. (2019) finds that June–September mean precipitation decreases by the end of the century (RCP8.5 scenario) in south-east Norway, but slightly increase along the West Coast of Southern Norway. EC-Earth shows a very similar pattern for October precipitation changes (see Fig. 2a, changes in 2 m temperature and IVT are shown in SI Fig. 7). Understanding precisely what drives this future precipitation change pattern is beyond the scope of this article, but we briefly attempt to quantify whether there are some changes in dynamics that could explain this drying in particular, since the CMIP5 models, and the Clausius-Clapeyron relationship, hint rather to a wettening (Hodnebrog et al., 2019).

Using the Weather Types (WT) classification from Otero et al. (2018), we quantify the changes in frequency of these WT for October in EC-Earth between present and future simulations. Haarsma et al. (2013) however provide a more formal evaluation of the model.

SI Fig. 8 shows that there are indeed some significant changes in WT occurring in our region of interest. The increase in Westerly flow is in line with an increase in precipitation along the northern side of the West Coast (perhaps strengthening the wettening expected from thermodynamics). Interestingly, there seems to be a strong increase in anticyclonic conditions in southern Norway at the same time, which is consistent with the drying in this region. The strong decrease in cyclonic conditions is more difficult to relate to the increase in precipitation in the northern part of the West Coast. However, precipitation does not only occur under cyclonic conditions hence this result is not necessarily

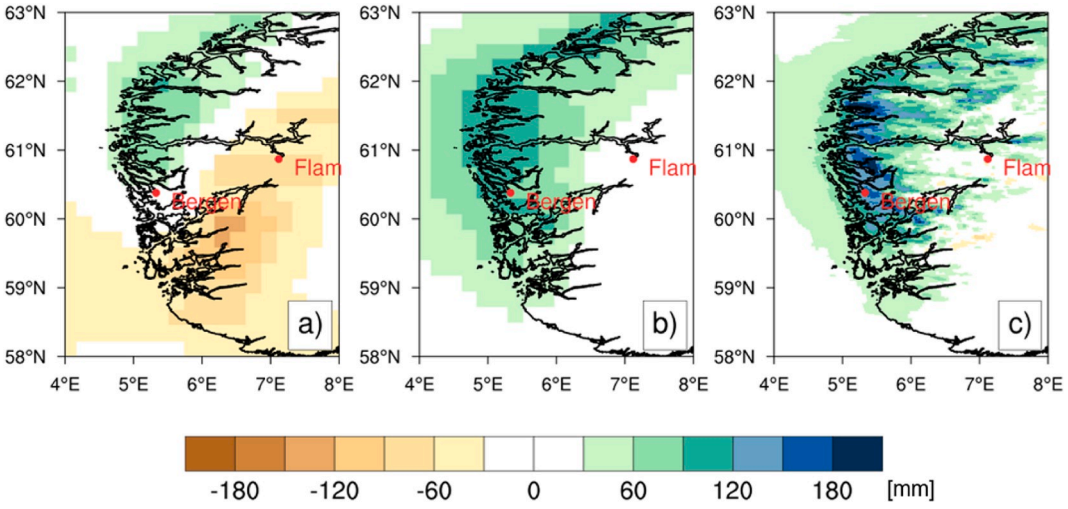

Fig. 2. Maps of the difference in a) 30 years October precipitation averages between PRESENT and FUTURE EC-Earth simulations, b) 144 h accumulated precipitation averaged over 10 ensemble members of the present and future EC-Earth reruns of the event and c) 144 h accumulated precipitation averaged over 10 ensemble members of the present and future AROME simulations of the event.

contradicting the other findings and more research would be needed to provide a proper interpretation. The results of the Westerly flow and Cyclonic conditions weather types are in line with Otero et al., 2018 (Fig. 5 in Otero et al., 2018) shows a similar pattern for SON in CMIP5), although the increase in Anticyclonic conditions is less pronounced in the southern part of Norway in CMIP5, potentially explaining why these models do not show a drying there.

The future precipitation event in this storyline study is wetter compared to the present one in both the EC-Earth reruns and AROME simulations over the western and northern parts of the West Coast of Norway, as shown in Fig. 2b and c. This is in line with both the facts that the intensity and frequency of ARs reaching the West Coast of Norway are expected to increase in the EC-Earth FUTURE simulations (Whan et al., 2019) and that most extreme precipitation events in the cold season are associated with ARs (Benedict et al., 2019a). It is also in line with the fact that despite the overall response of mean (or median) precipitation in the region being drying for October (see Figs. 2 and SI Fig. 4a, the higher percentiles of the distribution (95th, 99th and 99.99th) show more precipitation everywhere in the region in the future (shown as transects between 60°-61°N in SI Fig. 3b–d). We therefore seem to have captured this general response of extreme precipitation to global warming in that region with the present and future events we selected, as well as the fact that generally less precipitation reaches inland in the future in the case of ARs (Sandvik et al., 2018).

3.2. *Influence on the spatial resolution of the driving model*

The Norwegian operational flood-forecasting model (HBVlump) is used first to evaluate the effect of meteorological input data with higher horizontal resolution, i.e. an expected added-value of using AROME compared to EC-Earth, for the estimation of floods in the non-managed catchments of Norway. In this study, we focus on the Røykenes and Flåm catchments as discussed with stakeholders (see SI Fig. 1). The two catchments are interesting because they show a different response to the present and future AR's.

While considering the larger West Coast region defined in the previous section, EC-Earth's events were wetter compared to AROME (see Fig. 1), but when focusing on smaller catchment scales, this does not always hold. Whereas the precipitation is represented as one value over the entire catchment when using EC-Earth as input, valleys within the catchment can be either hit or not hit by precipitation when using AROME as input, as illustrated in SI Figs. 5–6 (lower 10 panels). For the two catchments selected in this study, we find that the precipitation and the resulting peak streamflows appears usually wetter for AROME than for EC-Earth (see Figs. 3–4). Another aspect is the difference in catchment average temperature between AROME and EC-Earth. For the present event in Flåm (see SI Fig. 9), the temperature modelled by AROME is about 1 °C warmer compared to EC-Earth. Whether the modelled temperature is below or above the melting point, as is the case in the present event in Flåm, will strongly affect the streamflows. The small streamflow response to precipitation of day 5 and 6 in Røykenes (Fig. 3) is clearly due to the low temperature (SI Fig. 9). In addition, with the steep topography of the region, differences in modelled precipitation and temperature at different elevations complicates the total estimations of streamflow.

In Røykenes, the future event is larger than the present one (see Fig. 3), which is in line with what one would expect for an extreme precipitation event in this region in a future climate (see previous section). For Flåm, however, the future event contains less precipitation and lower streamflow peaks than the present event for both the EC-Earth and the AROME (see Fig. 4). The Flåm catchment is not severely hit by the selected events, whereas the case of Røykenes exemplifies how the near coastal areas experience the highest increase in precipitation, which is in line with Sandvik et al. (2018). An evaluation of historical AR events shows that the development of the events and the area most severely hit varies between the events (e.g. Iden et al., 2005; Lussana et al., 2018; Stohl et al., 2008). Hegdahl et al. (2020) applied the AR events of this study to multiple catchments in the West Coast region and show that the future AR events cause more intense floods in more catchments than the present events. The overall impact is therefore

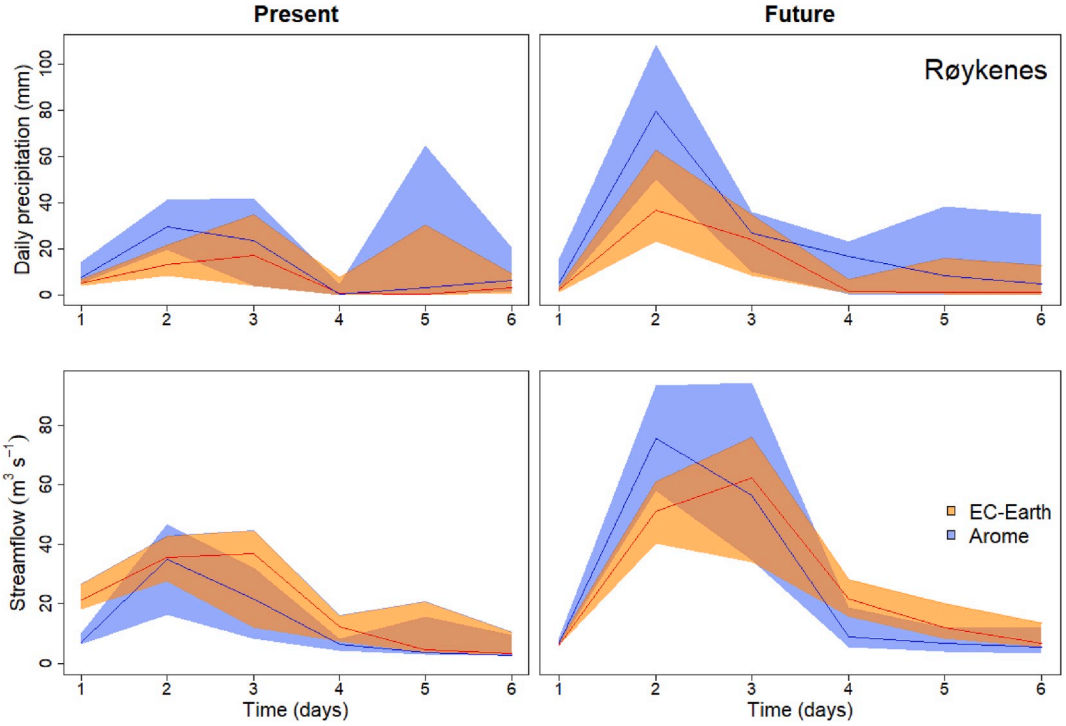

Fig. 3. Present (left) and future (right) events in the Røykenes catchment. The top panels show daily precipitation and the bottom ones, the streamflow. The shaded area represents the range of the 10 ensemble members for both EC-Earth (orange) and AROME (blue), with the lines within showing the median of the ten ensemble members. (For interpretation of the references to colour in this figure legend, the reader is referred to the Web version of this article.)

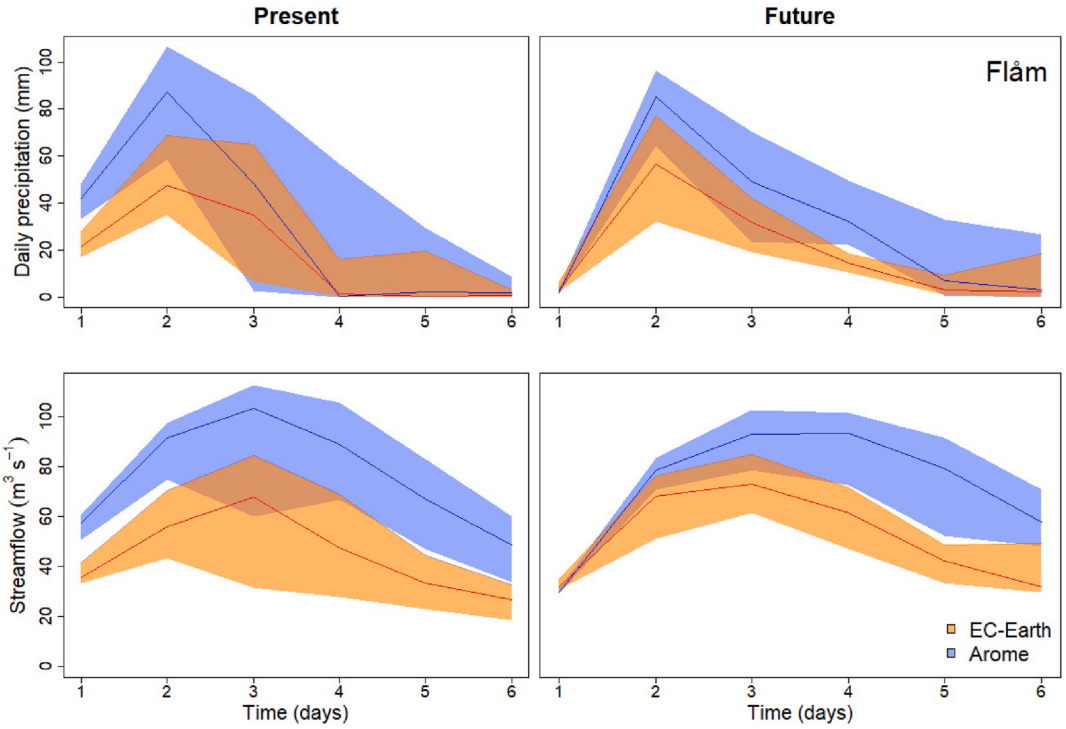

Fig. 4. Present (left) and future (right) events in the Flåm catchment. The top panels show daily precipitation and the bottom ones, the streamflow. The shaded area represents the range of the 10 ensemble members for both EC-Earth (orange) and AROME (blue), with the lines within showing the median of the ten ensemble members. (For interpretation of the references to colour in this figure legend, the reader is referred to the Web version of this article.)

higher for the future events than for present events, even though not all catchments are affected, as is the case for Flåm.

Figs. 3 and 4 further exemplify how combining AROME with a hydrological model is important to model the highest estimates of possible AR induced floods. AROME resolves the small-scale atmospheric processes, gives a better representation of orographic precipitation, and thereby provides an improved estimate for precipitation in relatively small and steep catchments, typical for the West Coast of Norway. The hydrological model describes the hydrological land process and estimates the hydrological initial conditions of the catchments that are important for the flood development. Besides precipitation, both snowmelt and soil moisture excess are drivers for floods (Beldring et al., 2008; Hegdahl et al., 2020; Sharma et al., 2018). Uncertainties related to the initial hydrological conditions are therefore discussed in the next section.

3.3. *Influence of the higher temporal resolution*

In this section, we are comparing streamflow simulations form the operational hydrological model set-up (HBVlump) to an alternative higher resolution distributed HBV model (HBVdist). HBVlump runs using daily temporal resolution, and precipitation and temperature data are averaged over the river catchment (268 km^2 for Flåm and 50 km^2 for Røykenes). HBVdist runs using hourly temporal resolution, and the input data are interpolated on a 1 × 1 km grid. A hydrological model running on a higher temporal resolution enables a better utilization of the available high-resolution temperature and precipitation data from AROME. From a theoretical perspective, the spatial distribution of precipitation is important because precipitation that falls in the upper areas of the catchment will take a longer time to contribute to the streamflow response than precipitation in the downstream area of the catchment. Similarly, the temporal resolution can influence the streamflow peak as higher intensity precipitation events can result in a quicker streamflow response.

Initial hydrologic conditions, such as the soil moisture or the snow depth, are important factors that influence the streamflow peak (e.g. Bengtsson et al., 2017). To sample the hydrological uncertainty of the flood simulations, HBVdist is rerun with 10 different initial conditions. Additionally, to sample hydrological parameter uncertainty, 10 parameter sets are selected during the calibration phase. Note that the uncertainty ranges in Figs. 5 and 6 represent this hydrological uncertainty, while the uncertainty range in Figs. 3 and 4 represented the 10 different ensemble members of each simulation.

To test this model framework, we run the HBVdist for the October 2014 flood, forced with temperature and precipitation from seNorge2 observations and from AROME simulations (Fig. 5). Note that the AROME simulations used here are the actual archived forecasts for 2014 and not the AROME climate simulations downscaling EC-Earth. Fig. 5 shows that the measured peak streamflow in Flåm is within the range of the streamflows modelled by HBVdist using both seNorge2 and the AROME actual forecasts. For the Flåm catchment, the streamflow simulation using both seNorge2 and AROME are similar and the measured streamflow is within the simulated hydrological uncertainty range, giving confidence in the ability of the modelling chain used in this study to simulate flood events.

We can only present this validation for HBVdist for the Flåm catchment, because seNorge2 hourly data does not extend back to 2005 and AROME was not operational in 2005. Thus, it is not possible to produce a similar validation for the September 2005 event in Røykenes.

Fig. 6 shows the streamflow simulations of HBVdist and HBVlump for Flåm and Røykenes. The same AROME temperature and precipitation input data is used for both hydrological models. For clarity, only the AROME ensemble member that causes the highest streamflow simulations is shown in Fig. 6, while again the range represents the uncertainty of the initial conditions and hydrological model parameters.

For the observed 2014 event, we find that the flood was building up over three days, with the highest peak generated over 5 h: from 12 to 17pm on October 28th. To realistically describe the responses of the catchments, hydrological models on sub-daily resolution are required. As expected, HBVdist simulates higher streamflow peaks than HBVlump

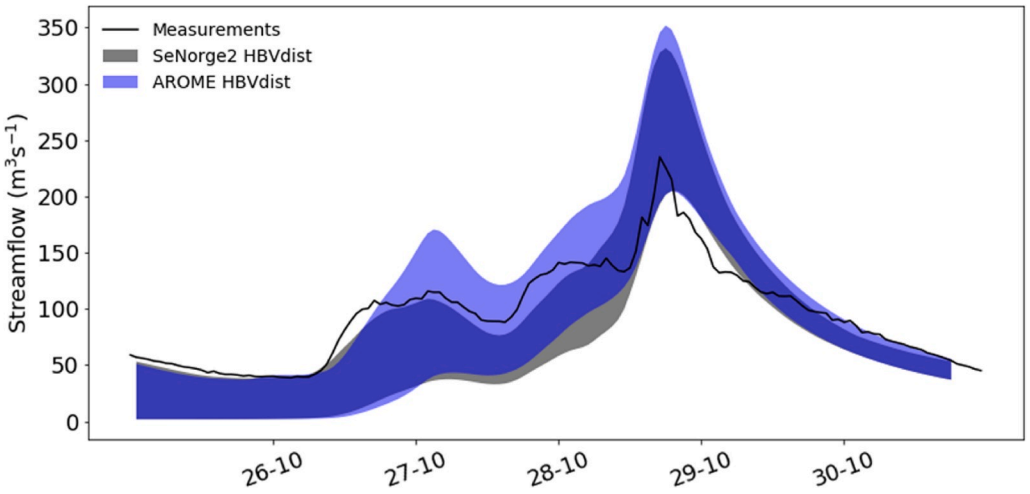

Fig. 5. Measured and HBVdist simulated streamflow for Flåm. The uncertainty range represents hydrologic uncertainty for the ensemble member with the highest peak streamflow.

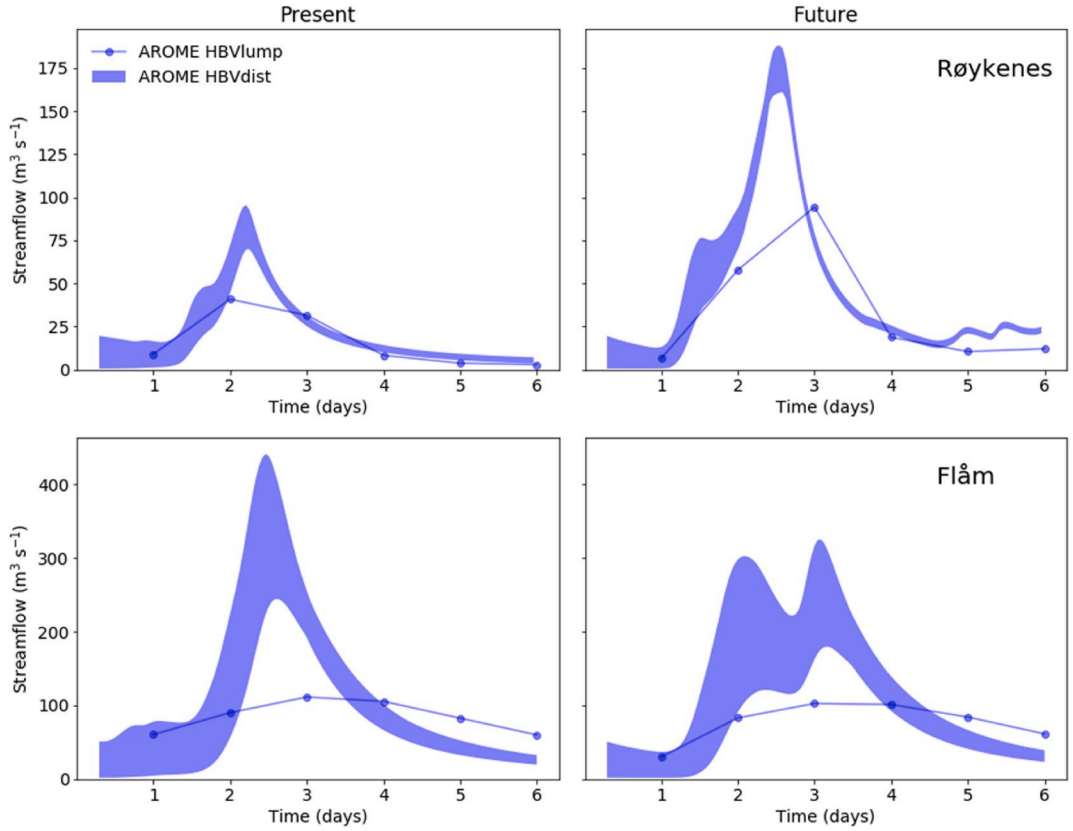

Fig. 6. The simulated streamflow for Røykenes (top) and Flåm (bottom), in the present (left) and future (right), using HBVlump and HBVdist. The HBVlump streamflow simulations are the same as in Fig. 5, but only the AROME present and future ensemble member resulting in the highest streamflow peak is shown. Similarly, for HBVdist, only the AROME present and future ensemble member that results in the highest streamflow peak are selected, and the uncertainty range represents hydrologic uncertainty (section 2.4).

for both the present and future events in both catchments. The simulations are 3–4 (Flåm) and 1 to 2 (Røykenes) times higher for HBVdist than HBVlump. The streamflow simulations show clearly the influence of hourly input in HBVdist showing more temporal variability than the HBVlump with daily input. For example, for Røykenes, the streamflow between the 2nd and 3rd day of the event is similar for HBVdist and HBVlump, whereas the peaks, occurring around 2.5 days, are much higher for HBVdist. The hourly peak compared to the daily peak for Røykenes is within the expected values when looking up the factor used to estimate the flood culmination value based on the daily flood value. For Flåm, however, the difference between hourly and daily peak is too large and therefore it is difficult to compare the results directly. The large discrepancy between the HBVdist and HBVlump could be caused by the fact that the models are calibrated on different versions of the seNorge dataset. The hourly data are available for a shorter period and less quality checked than the daily data and different interpolation

methods are applied that affect the precipitation (v2.0 has less precipitation amounts than v1.1). Both can have a large effect on the tuning of hydrological model parameters (connected to precipitation) and thereby the estimation of floods.

In the previous section it was shown that the local, catchment-scale impact can be less in future events compared to present events depending on the catchment. This effect was predominantly found for the AROME events, because the high-resolution weather forecast model shows more spatial variability than the higher resolution EC-Earth model. The fact that some catchments might and others might not be hit by a precipitation event is consistent with streamflow observations of the 2014 event, which show that Flåm was hit but Røykenes, among others, was not (SI Fig. 10). As mentioned before, Fig. 6 shows only the AROME event resulting in the highest streamflow rather than the average of the 10 events, but leads to the same conclusions drawn from Figs. 3 and 4. That is, peak streamflows in Røykenes are higher in the future compared to present, whereas in the Flåm catchment, the future event is weaker than in present. The future event in Røykenes shows an almost two-fold increase in streamflow at peak-time in addition to extending over a longer period of time (Fig. 6). The peak streamflow of ca. 180 m^3/s^1 of this event is ca. 20% higher compared to the largest flood event ever measured in this catchment, a flood in 1953 with a streamflow peak of ca. 140 m^3/s^1 (Væringstad, 2014).

4. Conclusions

After consulting a range of users and stakeholders, the autumn floods of September 2005 and October 2014, both caused by an atmospheric river hitting the West Coast of Norway, were chosen as a typical event for this physical climate storyline study. In particular, we investigate the impact of having higher spatial (from 25 km in EC-Earth to 2.5 km in AROME) and temporal resolution (daily vs. hourly) for the simulation of peak flows in two catchments. In addition, we are using a modelling chain that mimics as closely as possible the operational modelling chain for flood warnings in Norway.

We first show that the present event is realistically simulated by both EC-Earth and AROME when looking at a larger region in the West Coast of Norway. EC-Earth's events are also slightly wetter than in AROME, but this is likely an artefact of the different resolutions. AROME shows stronger local peaks in precipitation but also some locations appear to receive almost no precipitation during the event, which is plausible in such a mountainous area. EC-Earth, in contrast, shows more homogenous precipitation amounts for the larger grid cells and misses the fact that extreme precipitation actually falls in a more localised manner. The high resolution of the EC-Earth simulations (compared to e.g. CMIP5 climate models) allow for more realistic atmospheric circulation patterns (e.g. van Haren et al., 2015), but for applications studied here, the resolution is insufficient. Downscaling with AROME is necessary to obtain more realistic precipitation distributions. In both EC-Earth and AROME however, there are differences between the 10 ensemble members, which can likely be traced back to where the atmospheric river is located, and how intense it is in the perturbed EC-Earth reruns. The difference between present and future events follow overall the expectation that extreme precipitation will mostly increase in this region in Autumn (Hanssen-Bauer et al., 2017), while mean precipitation is expected to decrease in the south and increase on the northern West Coast. Whan et al. (2019)'s results suggest that this increase in extreme precipitation is caused by more intense and frequent atmospheric rivers hitting the region in the future in October–March, which should be taken into account in future adaptation planning in the region.

We then investigate the local impact on two catchments at the West Coast of Norway: Flåm and Røykenes. Whereas EC-Earth appears overall wetter when considering the larger region of the West Coast of Norway, we find that AROME produces more precipitation (in terms of intensity and quantity) for the two studied catchments. Translating this to physical impacts, the AROME simulations result in higher peak streamflows compared to EC-Earth. The difference between present and future events shows a future increase in streamflow for Røykenes, and a decrease for Flåm. This result is consistent for the two hydrological model versions analysed, with the higher resolution model simulating even larger peak streamflows. Previous studies also showed that for the West Coast, autumn peak streamflow is expected to become stronger with precipitation increases in a warmer climate (Beldring, 2008; Hanssen-Bauer et al., 2017; Lawrence and Hisdal, 2011; Sorteberg et al., 2018; Vormoor et al., 2015). The unexpected result that the future events in Flåm have less physical impact (i.e. less streamflow) is likely due to the fact that the future event did not hit Flåm. Even though the streamflow peaks are on average higher in a future climate, not every future event will hit every catchment. We attempted to take into account the uncertainty regarding which catchments are hit by perturbing each selected event ten times (see section 2). Our selected cases cannot span the entire range of possibilities where an AR reaches the coast of Norway or its passage over land, but we can go into much more detail for a specific case. Physical climate storylines should be viewed as "what if" scenarios that can provide insights, for instance for emergency preparedness, even if the probability of that event is unknown or very unlikely, and to study possible impacts associated with such an event. Physical climate storylines can be used to reveal complexity and uncertainties in the system that cannot be revealed in a coarser, more probabilistic focused approach.

Overall, Hegdahl et al. (2020), found that the future events cause larger floods coinciding in many more catchments compared to the present events, which underlines that the severity of an event may not necessarily be captured in a single catchment analysis. We find that hourly timescales (instead of daily) represent the fast flood-generating processes in these catchments better and therefore provide a more realistic temporal evolution of the flood event, capturing higher peak flood intensities. We conclude that especially in a mountainous region such as the West Coast of Norway, higher spatial and temporal resolutions in both the climate and hydrological models lead to more realistic estimations of the potential peak floods, which is important information for users, such as NVE. Another valuable aspect of physical climate storylines is the familiarity of the operational setup and data format for the users. NVE and Statkraft could both easily use the data produced.

When considering individual events as is the case in a storyline approach, it is obviously impossible to make any statements about their probability of occurrence. It is however possible to put them in context of expected future climate change from other GCM ensembles such as CMIP5 or from the literature, as we did here. Also, it is possible to study the dynamics of the event and possible compounded effects in detail, which are often obscured in probabilistic projections. At the same time, it is also key to communicate that each event is unique, and no general "projection" can be obtained from a storyline approach. In addition, communicating different outcomes for different catchments to the users, and in our case, the counterintuitive results that the future event in Flåm is weaker compared to the present one, is not an easy task. The community needs to be aware that physical climate storylines studies might not always lead to the expected results, but having the users involved from the design of the storyline until the interpretation of results can support mutual understanding of the process and challenges involved. Further studies are needed to better understand the added value of a physical climate storyline approach for users, such as municipalities challenged with making decision for adaptation measures for future climate change (Bremer et al., 2019; Cortes Arevalo et al., 2018; de Bruijn et al., 2016).

Physical modelling supporting a storyline approach is a relatively new field of research in the physical climate change community and a lot of research is ongoing and needed (Sillmann et al., 2019). We briefly summarise here a few key aspects discovered in this study that require further research:

1) As in probabilistic event attribution, the definition of the event is highly important (Otto et al., 2015). For example, in hindsight it is clear that the selection criteria for the event in the EC-Earth PRESENT and FUTURE simulations (i.e. 24 h accumulated precipitation) could have been optimized by considering longer event duration (e.g. 3 days) which will likely affect the results obtained further down in the modelling chain. Sensitivity analysis could be done given sufficient computational resources that were not available for this study. However, our study was able to show that high spatial resolution throughout the model chain (including the global climate model) is needed for realistically simulating the magnitude of AR events and associated floods.
2) As Felder et al. (2018) also discuss, there is no guarantee that the chosen event in the GCM will correspond to an extreme event once downscaled. The catchment of Flåm is clearly not much affected in the future event, leading to the fact that the present event appears stronger, which is not trivial to communicate with the users.
3) We performed 10 re-runs with the driving GCM before doing the downscaling, using one way of perturbing the initial conditions, but more research should be done on this to know how important internal variability is. We chose 10 ensemble members as a trade-off between computing capacity and representation of internal variability, but there is no physical or statistical reason beyond this.
4) In our region of interest, the West Coast of Norway, temperature is important for the partitioning between snow and rain, and snowmelt when there is snow in the catchment. The flood development during cold seasons are therefore also depending on temperature. If precipitation falls and is stored as snow, it will not contribute to streamflow. In this study we focussed on October when temperatures are usually still above the freezing point. The impact of a future change in temperature is not only important to the amount of precipitation reaching western Norway, but also for the phase of the precipitation (Poschlod et al., 2020). A winter AR which today deposits snow at higher elevations can in a warmer climate cause floods (Whan et al., 2019).

Declaration of competing interest

The authors declare no conflict of interests.

CRediT authorship contribution statement

Nathalie Schaller: Methodology, Validation, Formal analysis, Investigation, Resources, Data curation, Writing - original draft, Visualization. **Jana Sillmann:** Conceptualization, Methodology, Writing - original draft, Writing - review & editing, Supervision, Project administration, Funding acquisition. **Malte Müller:** Conceptualization, Methodology, Validation, Formal analysis, Investigation, Resources, Data curation, Writing - original draft, Writing - review & editing, Visualization, Supervision, Funding acquisition. **Reindert Haarsma:** Conceptualization, Methodology, Validation, Investigation, Resources, Data curation, Writing - original draft. **Wilco Hazeleger:** Conceptualization, Methodology, Writing - review & editing, Project administration, Funding acquisition. **Trine Jahr Hegdahl:** Methodology, Validation, Formal analysis, Investigation, Resources, Data curation, Writing - original draft, Visualization. **Timo Kelder:** Methodology, Validation, Formal analysis, Investigation, Resources, Data curation, Writing - original draft, Visualization. **Gijs van den Oord:** Methodology, Validation. **Albrecht Weerts:** Methodology, Writing - review & editing, Supervision. **Kirien Whan:** Methodology, Validation, Formal analysis, Writing - review & editing, Visualization.

Acknowledgement

This study has received support from the project TWEX (255037) and TWEX-film (304551) funded through the Research Council of Norway.

We thank Noelia Otero for her help with calculating the weather types.

Appendix A. Supplementary data

Supplementary data to this article can be found online at https://doi.org/10.1016/j.wace.2020.100259.

References

Azad, R., Sorteberg, A., 2017. Extreme daily precipitation in coastal western Norway and the link to atmospheric rivers. J. Geophys. Res. Atmos. 122, 2080–2095. https://doi.org/10.1002/2016JD025615.

Beldring, S., 2008. Distributed element water balance model system. NVE Report 2008, 42pp, 4. http://publikasjoner.nve.no/report/2008/report2008_04.pdf.

Beldring, S., Engen-Skaugen, T., Førland, E.J., Roald, L.A., 2008. Climate change impacts on hydrological processes in Norway based on two methods for transferring regional climate model results to meteorological station sites. Tellus Dyn. Meteorol. Oceanogr. 60 (3), 439–450.

Benedict, I., Ødemark, K., Nipen, T., Moore, R., 2019a. Large-scale flow patterns associated with extreme precipitation and atmospheric rivers over Norway. Mon. Weather Rev. https://doi.org/10.1175/MWR-D-18-0362.1.

Benedict, I., van Heerwaarden, C.C., Weerts, A.H., Hazeleger, W., 2019b. The benefits of spatial resolution increase in global simulations of the hydrological cycle evaluated for the Rhine and Mississippi basins. Hydrol. Earth Syst. Sci. 23, 1779–1800. https://doi.org/10.5194/hess-23-1779-2019.

Bengtsson, L., Andrae, U., Aspelien, T., Batrak, Y., Calvo, J., de Rooy, W., Gleeson, E., Hansen-Sass, B., Homleid, M., Hortal, M., Ivarsson, K.-I., Lenderink, G., Niemelä, S., Nielsen, K.P., Onvlee, J., Rontu, L., Samuelsson, P., Santos Muñoz, D., Subias, A., Tijm, S., Toll, V., Yang, X., Køltzow, M.Ø., 2017. The HARMONIE–AROME model configuration in the ALADIN–HIRLAM NWP system. Mon. Weather Rev. 145, 1919–1935. https://doi.org/10.1175/MWR-D-16-0417.1.

Bergström, S., 1976. Development and application of a conceptual runoff model for Scandinavian catchments. In: SMHI RHO, vol. 7. Norrköping.

Bremer, S., Wardekker, A., Dessai, S., Sobolowski, S., Slaattelid, R., van der Sluijs, J., 2019. Toward a multi-faceted conception of co-production of climate services. Climate Services 13, 42–50. https://doi.org/10.1016/j.cliser.2019.01.00.

Cortes Arevalo, V.J., Verbrugge, L.N.H., Haan, R.-J. d., Baart, F., van der Voort, M.C., Hulscher, S.J.M.H., 2018. Users' perspectives about the potential usefulness of online storylines to communicate river research to a multi-disciplinary audience. Environ. Commun. 13 (7), 909–925. https://doi.org/10.1080/17524032.2018.1504098.

de Bruijn, K.M., Lips, N., Gersonius, B., Middelkoop, H., 2016. The storyline approach: a new way to analyse and improve flood event management. Nat. Hazards 81 (1), 99–121. https://doi.org/10.1007/s11069-015-2074-2.

Dee, D.P., et al., 2011. The ERA-Interim reanalysis: configuration and performance of the data assimilation system. Q. J. R. Meteorol. Soc. 137, 553–597.

Dyrrdal, A.V., Skaugen, T., Stordal, F., Førland, E.J., 2016. Estimating extreme areal precipitation in Norway from a gridded dataset. Hydrol. Sci. J. 61, 483–494. https://doi.org/10.1080/02626667.2014.947289.

Felder, G., Gómez-Navarro, J.J., Zischg, A.P., Raible, C.C., Röthlisberger, V., Bozhinova, D., Martius, O., Weingartner, R., 2018. From global circulation to local flood loss: coupling models across the scales. Sci. Total Environ. 635, 1225–1239. https://doi.org/10.1016/j.scitotenv.2018.04.170.

Haarsma, R.J., Hazeleger, W., Severijns, C., de Vries, H., Sterl, A., Bintanja, R., van Oldenborgh, G.J., van den Brink, H.W., 2013. More hurricanes to hit western Europe due to global warming. GRL 40 (9), 1783–1788.

Hanssen-Bauer, I., Førland, E.J., Haddeland, I., Hisdal, H., Mayer, S., Nesje, A., Nilsen, J. E.Ø., Sandven, S., Sandø, A.B., Sorteberg, A., Ådlandsvik, B., 2017. Climate in Norway 2100 - a Knowledge Base for Climate Adaption. NCCS Report 1/2017. https://www.miljodirektoratet.no/globalassets/publikasjoner/M741/M741.pdf.

van Haren, R., Haarsma, R.J., van Oldenborgh, G.J., Hazeleger, W., 2015. Resolution dependence of European precipitation in a state-of-the-art atmospheric general circulation model. J. Clim. 28.

Hazeleger, W., et al., 2010. EC-earth A seamless earth-system prediction approach in action. BAMS. https://doi.org/10.1175/2010BAMS2877.1.

Hazeleger, W., van den Hurk, B.J.J.M., Min, E., van Oldenborgh, G.J., Petersen, A.C., Stainforth, D.A., Vasileiadou, E., Smith, L.A., 2015. Tales of future weather. Nat. Clim. Change 5. https://doi.org/10.1038/NCLIMATE2450.

Hegdahl, Trine, Engeland, Kolbjørn, Müller, Malte, Sillmann, Jana, 2020. An event-based approach to explore selected present and future Atmospheric River induced floods in western Norway. Journal of Hydrometeorology. https://doi.org/10.1175/JHM-D-19-0071.1.

Hodnebrog, Ø., Marelle, L., Alterskjær, K., Wood, R.R., Ludwig, R., Fischer, E.M., Richardson, T.B., Forster, P.M., Sillmann, J., Myhre, G., 2019. Future changes in mean and extreme summer precipitation over Europe. ERL 14, 124050.

Houska, T., et al., 2015. Spotting model parameters using a ready-made python package. In: Langsholt, E., Roald, L.A., Holmqvist, E., Fleig, A. (Eds.), 2015. Flommen På Vestlandet Oktober 2014. NVE Rapport Nr 112015.

van den Hurk, B.J.J.M., Viterbo, P., Beljaars, A.C.M., Betts, A.K., 2000. Offline validation of the ERA40 surface scheme. ECMWF TechMemo 295. http://www.ecmwf.int/publications/library/ecpublications/pdf/tm/001-300/tm295.pdf.

Iden, K, Isaksen, K, Kristiansen, S, Szewczyk-Bartnicka, H, 2005. Weather in Norway-Climatological monthly overview for September 2005.), met.no.info (09/2005), Meteorological Institute, Oslo, Norway. ISSN 1503-8017.

Jacob, D., et al., 2014. EURO-CORDEX: new high-resolution climate change projections for European impact research. Reg. Environ. Change 14, 563–578.

Lawrence, D., Hisdal, H., 2011. Hydrological projections for floods in Norway under a future climate. Nor. Water Resour. Energy Dir. Rep. 2011 (5). ISBN: 978-82-410-0753-8.

Lussana, C., Saloranta, T., Skaugen, T., Magnusson, J., Tveito, O.E., Andersen, J., 2018. seNorge2 daily precipitation, an observational gridded dataset over Norway from 1957 to the present day. Earth Syst. Sci. Data 10, 235–249. https://doi.org/10.5194/essd-10-235-2018.

Mohr, M., 2008. New Routines for Gridding of Temperature and Precipitation Observations for "seNorge. No". MET report No 08/2008, available at. ftp://ftp.met.no/projects/klimagrid/doc/NewRoutinesforGriddingofTemperature.pdf.

Mohr, M., 2009. Comparison of Versions 1.1 and 1.0 of Gridded Temperature and Precipitation Data for Norway. MET report No 19/2009, available at. ftp://157.249.32.246/projects/klimagrid/doc/Comparison%20of%20versions%201.1%20and%201.0%20of%20gridded%20climate%20data.pdf.

Müller, M., Homleid, M., Ivarsson, K.-I., Køltzow, M.A.Ø., Lindskog, M., Midtbø, K.H., Andrae, U., Aspelien, T., Berggren, L., Bjørge, D., Dahlgren, P., Kristiansen, J., Randriamampianina, R., Ridal, M., Vignes, O., 2017. AROME-MetCoOp: a Nordic convective-scale operational weather prediction model. Weather Forecast. 32, 609–627. https://doi.org/10.1175/WAF-D-16-0099.1.

Nash, J.E., Sutcliffe, J.V., 1970. River flow forecasting through conceptual models part i—a discussion of principles. J. Hydrol. 10 (3), 282–290.

Otero, Noelia, Sillmann, Jana, Butler, Tim, 2018. Assessment of an extended version of the Jenkinson-Collison classification on CMIP5 models over Europe. Climate Dynamics 50. https://doi.org/10.1007/s00382-017-3705-y.

Otto, F.E.L., Boyd, E., Jones, R.G., Cornforth, R.J., James, R., Parker, H.R., Allen, M.R., 2015. Attribution of extreme weather events in Africa: a preliminary exploration of the science and policy implications. Climatic Change. https://doi.org/10.1007/s10584-015-1432-0.

Porter, J.J., Dessai, S., 2017. Mini-me: why do climate scientists' misunderstand users and their needs? Environ. Sci. Pol. 77, 9–14.

Poschlod, B., Zscheischler, J., Sillmann, J., Wood, R.R., Ludwig, R., 2020. Climate change effects on hydrometeorological compound events over southern Norway. Weather. Clim. Extr. 28, 100254.

Prein, A.F., et al., 2015. A review on regional convection-permitting climate modeling: demonstrations, prospects, and challenges. Rev. Geophys. 53, 323–361.

Rogelj, J., Meinshausen, M., Knutti, R., 2012. Global warming under old and new scenarios using IPCC climate sensitivity range estimates. Nat. Clim. Change 2, 248–253. https://doi.org/10.1038/nclimate1385.

Sælthun, N.R., 1996. The Nordic HBV model. Nor. Water Resour. Energy Dir. 7, 1–26.

Sandvik, M.I., Sorteberg, A., Rasmussen, R., 2018. Sensitivity of historical orographically enhanced extreme precipitation events to idealized temperature perturbations. Clim. Dynam. 50, 143–157. https://doi.org/10.1007/s00382-017-3593-1.

Schaller, N., Kay, A.L., Lamb, R., Massey, N.R., van Oldenborgh, G.J., Otto, F.E.L., Sparrow, S.N., Vautard, R., Yiou, P., Ashpole, I., Bowery, A., Crooks, S.M., Haustein, K., Huntingford, C., Ingram, W.J., Jones, R.G., Legg, T., Miller, J., Skeggs, J., Wallom, D., Weisheimer, A., Wilson, S., Stott, P.A., Allen, M.R., 2016. Human influence on climate in the 2014 Southern England winter floods and their impacts. Nat. Clim. Change 6 (6).

Schellekens, J., van Verseveld, W., de Boer-Euser, T., Winsemius, H., Thiange, C., Bouaziz, L., Tollenaar, D., de Vries, S., Weerts, A.H., 2017. Openstreams wflow documentation. available at: https://wflow.readthedocs.io/en/stable/. .

Sharma, A., Wasko, C., Lettenmaier, D.P., 2018. If precipitation extremes are increasing, why aren't floods? Water Resour. Res. 54, 8545–8551.

Shepherd, T.G., 2019. Storyline approach to the construction of regional climate change information. Proc. R. Soc. A 475, 20190013. https://doi.org/10.1098/rspa.2019.0013.

Shepherd, T.G., Boyd, E., Calel, R.A., Chapman, S.C., Dessai, D., Dima-West, I.M., Fowler, H.J., James, R., Maraun, D., Martius, O., Senior, C.A., Sobel, A.H., Stainforth, D.A., Tett, S.F.B., Trenberth, K.E., van den Hurk, B.J.J.M., Watkins, N.W., Wilby, R.L., Zenghelis, D.A., 2018. Storylines: an alternative approach to representing uncertainty in physical aspects of climate change. Climatic Change 151, 555–571.

Sillmann, J., Kharin, V.V., Zwiers, F.W., Zhang, X., Bronaugh, D., 2013. Climate extremes indices in the CMIP5 multimodel ensemble: Part 2. Future climate projections. J. Geophys. Res. Atmos. 118, 2473–2493. https://doi.org/10.1002/jgrd.50188.

Sillmann, J., Shepherd, T., van den Hurk, B., Hazeleger, W., Martius-Rompainen, O., Zscheischler, J., 2019. Physical modeling supporting a storyline approach. CICERO Policy Note 2019:01, available at: https://www.cicero.oslo.no/en/publications-and-events_twex/workshop-on-physical-modeling-supporting-a-storyline-approach.

Sodemann, H., Stohl, A., 2013. Moisture origin and meridional transport in atmospheric rivers and their association with multiple cyclones. Mon. Weather Rev. 141, 2850–2868. https://doi.org/10.1175/MWR-D-12-00256.1.

Sorteberg, A., Lawrence, D., Dyrrdal, A.V., Mayer, S., Engeland, K. (Eds.), 2018. Climate Changes in Short Duration Extreme Precipitation and Rapid Onset Flooding – Implications for Design Values. Norwegian Center for Climate Services. NCCS Report 2018:1, available at: https://cms.met.no/site/2/klimaservicesenteret/rapporter-og-publikasjoner/_attachment/13537?_ts=163df95ff7b.

Sterl, A., Severijns, C., Dijkstra, H., Hazeleger, W., van Oldenborgh, G.J., van den Broeke, M., Burgers, G., van den Hurk, B., van Leeuwen, P.J., van Velthoven, P., 2008. When can we expect extremely high surface temperatures? Geophys. Res. Lett. 35, L14703.

Stohl, A., Forster, C., Sodemann, H., 2008. Remote sources of water vapor forming precipitation on the Norwegian West Coast at 60°N—a tale of hurricanes and an atmospheric river. J. Geophys. Res. 113, D05102. https://doi.org/10.1029/2007JD009006.

Swedish Meteorological and Hydrological Institute, 2014. IHMS - Integrated Hydrological Modelling System. Manual version 6.4.

Taylor, K.E., Stouffer, R.J., Meehl, G.A., 2012. An overview of CMIP5 and the experiment design. Bull. Am. Meteorol. Soc. 93, 485–498.

Væringstad, T., 2014. Flomberegning for Nesttunvassdraget (056.3Z), Rapport Nr. 16 – 2014. NVE Report, available at: http://publikasjoner.nve.no/rapport/2014/rapport2014_16.pdf.

Vormoor, K., Lawrence, D., Heistermann, M., Bronstert, A., 2015. Climate change impacts on the seasonality and generation processes of floods – projections and uncertainties for catchments with mixed snowmelt/rainfall regimes. Hydrol. Earth Syst. Sci. 19, 913–931. https://doi.org/10.5194/hess-19-913-2015.

van Vuuren, D.P., Edmonds, J., Kainuma, M., Riahi, K., Thomson, A., Hibbard, K., Hurtt, G.C., Kram, T., Krey, V., Lamarque, J.F., Masui, T., Meinshausen, M., Nakicenovi, N., Smith, S.J., Rose, S.K., 2011. The representative concentration pathways: an overview. Climatic Change 109, 5–31.

Werner, M., Schellekens, J., Gijsbers, P., van Dijk, M., van den Akker, O., Heynert, K., 2013. The Delft-FEWS flow forecasting system. Environ. Model. Software 40, 65–77. https://doi.org/10.1016/j.envsoft.2012.07.010.

Whan, K., Sillmann, J., Schaller, N., Haarsma, R., 2019. Future changes in atmospheric rivers and extreme precipitation in Norway. Clim. Dynam. 54, 2071–2084.